Catalysis-reduction strategy for sensing inorganic and organic mercury based on gold nanoparticles

Article *in* Biosensors & Bioelectronics · November 2016

DOI: 10.1016/j.bios.2016.10.097

6 authors, including:

Youlin Zhang
Chinese Academy of Sciences
58 PUBLICATIONS **1,205** CITATIONS
SEE PROFILE

Yulei Chang
Changchun Institute of Optics, Fine Mechanics and Physics
36 PUBLICATIONS **418** CITATIONS
SEE PROFILE

Bin Xue
Chinese Academy of Sciences
26 PUBLICATIONS **136** CITATIONS
SEE PROFILE

Wei Chen
Chinese Academy of Sciences
58 PUBLICATIONS **3,031** CITATIONS
SEE PROFILE

Biosensors and Bioelectronics 92 (2017) 328–334

Contents lists available at ScienceDirect

Biosensors and Bioelectronics

journal homepage: www.elsevier.com/locate/bios

Catalysis-reduction strategy for sensing inorganic and organic mercury based on gold nanoparticles

Xiaokun Li[a,b], Youlin Zhang[a,*], Yulei Chang[a], Bin Xue[a], Xianggui Kong[a,*], Wei Chen[b,*]

[a] State Key Laboratory of Luminescence and Applications, Changchun Institute of Optics, Fine Mechanics and Physics, Chinese Academy of Sciences, Changchun 130033, China

[b] State Key Laboratory of Electroanalytical Chemistry, Changchun Institute of Applied Chemistry, Chinese Academy of Sciences, Changchun 130022, China

ARTICLE INFO

Keywords:
Gold nanoparticle
AuNP catalysis
Detection
Mercury

ABSTRACT

In view of the high biotoxicity and trace concentration of mercury (Hg) in environmental water, developing simple, ultra-sensitive and highly selective method capable of simultaneous determination of various Hg species has attracted wide attention. Here, we present a novel catalysis-reduction strategy for sensing inorganic and organic mercury in aqueous solution through the cooperative effect of AuNP-catalyzed properties and the formation of gold amalgam. For the first time, a new AuNP-catalyzed-organic reaction has been discovered and directly used for sensing Hg^{2+}, Hg_2^{2+} and CH_3Hg^+ according to the change of the amount of the catalytic product induced by the deposition of Hg atoms on the surface of AuNPs. The detection limit of Hg species is 5.0 pM (1 ppt), which is 3 orders of magnitude lower than the U.S. Environmental Protection Agency (EPA) limit value of Hg for drinking water (2 ppb). The high selectivity can be exceptionally achieved by the specific formation of gold amalgam. Moreover, the application for detecting tap water samples further demonstrates that this AuNP-based assay can be an excellent method used for sensing mercury at very low content in the environment.

1. Introduction

Mercury (Hg) has been widely recognized as one of the most hazardous pollutant and highly dangerous element because of its accumulative and toxic properties in the ecological system (Schrope, 2001). Mercury presents a variety of combined forms in environment, including inorganic mercury (Hg^{2+} and Hg_2^{2+}) and organic mercury (such as CH_3HgX, X=Cl^-, Br^-, AcO^-, etc.) (Nolan and Lippard, 2008). Although Hg^{2+} is the main existing form in natural water, all inorganic mercury released into the ecosystem can be eventually converted to organic forms by microorganisms or microalgae in aquatic environments (Lehnherr et al., 2011). And organic mercury has much higher toxicity than inorganic forms due to their high liposolubility in the food chain (Jensen and Jermelov, 1969; Boening, 2000). Therefore, an important and challenging task in the scientific community is to design and develop ultrasensitive detection methods for Hg species in water samples to reduce or avoid the threat of Hg to human health (Nolan and Lippard, 2008).

In principle, the conventional approaches, such as atomic absorption spectroscopy (AAS) and inductively coupled plasma-mass spectrometry (ICP-MS) (Yan et al., 2003; Gao et al., 2012; Hong et al., 2011), can measure the total Hg content with a satisfying sensitivity. However, the disadvantages of these methods are obvious that they require complicated, multistep sample preparation and sophisticated instruments, which all limit the applications of these methods for Hg detection.

In order to conveniently and efficiently sense Hg species, various detection strategies have been developed, in which, optical methods (Kim et al., 2012), such as fluorescence (Ding et al., 2016; Bera et al., 2014), chemosensors (Zapata et al., 2009; Cai et al., 2011), and colorimetric assays (Chen et al., 2014a, 2014b; Lee et al., 2007), have been regarded as the most attractive tools due to the simplicity and high sensitivity. The detecting mechanisms of these methods are almost to use the receptors to recognize the targeted metal ions based on the principles of traditional coordination or host-guest chemistry, which makes the optical methods have two universal drawbacks for sensing Hg: 1) Most methods aim at one of the Hg species (Hg^{2+} or organic mercury), and no method is used for Hg_2^{2+} detection maybe because it is difficult to obtain appropriate receptors to effectively interact with Hg_2^{2+}. Thus the detection results only represent partial Hg content rather than total Hg content in samples, which is a potential hazardous issue. 2) Most methods are not sensitive enough to apply in

* Corresponding authors.
E-mail addresses: zhangyl@ciomp.ac.cn (Y. Zhang), kongxg14@ciomp.ac.cn (X. Kong), weichen@ciac.ac.cn (W. Chen).

http://dx.doi.org/10.1016/j.bios.2016.10.097
Received 2 August 2016; Received in revised form 18 October 2016; Accepted 28 October 2016
Available online 05 November 2016
0956-5663/

real water samples, although the detection limits of these assays are from nM to μM range. In view of low concentration but high toxicity of Hg in aquatic environment, the U.S Environmental Protection Agency (EPA) has set the maximum allowable level of Hg in drinking water at 10 nM (2 ppb) (EPA, 2001). Therefore, the detection methods with detection limits in the pM (ppt) to low-nM (ppb) range are highly desirable to analyze Hg species. Although there are some reports that can detect Hg^{2+} with ultra-sensitivity (Bera et al., 2014), or simultaneously detect both Hg^{2+} and organomercury (Shu et al., 2015; Chen et al., 2010; Santra et al., 2009). However, to our knowledge, the optical method for simultaneously detecting various Hg species with a pM magnitude in aqueous solution has not been previously reported.

Gold nanoparticles (AuNPs), as one of optical probes, have been widely used to detect metal ions due to their attractive optical properties (Wang and Ma, 2009; Du et al., 2013; Lee and Mirkin, 2008; Xue et al., 2008; Huang and Chang, 2007; Liu and Lu, 2003; Zhou et al., 2008; Li et al., 2010). However, most of these assays based on functionalized AuNPs face with the same drawbacks as other optical methods. In fact, from the perspective of nanoparticle applications, the attempt of exploring the inherent properties of AuNPs e.g. their surface properties, instead of using the properties of functional molecules on their surface for detecting analytes, may bring breakthrough in sensing methodology and mechanism for Hg species.

AuNP catalysis, using the surface properties of AuNPs, has attracted continuous interests because of its potential applications in many organic reactions (Arcadi, 2008; Zhang et al., 2012; Panigrahi et al., 2007; Comotti et al., 2004). The previous research demonstrates the catalytic efficiency is extremely sensitive to the surface properties of AuNPs (Arcadi, 2008). A little surface morphology change may significantly affect the catalytic performance of AuNPs. In addition, in an Au-Hg mixed system, the Hg° exhibits a strong affinity to clean AuNP surface due to forming Au amalgam, which can be used to distinguish Hg species from other general metal ions to ensure the specificity based on AuNPs. Therefore, combining AuNP-catalyzed properties with Au amalgam for sensing Hg species with a desired performance is greatly possible. In fact, some articles have reported that the peroxidase-like catalytic activities of AuNPs could be used to detect metal ions (Lien et al., 2014; Wang et al., 2012; Tseng et al., 2012). In these cases, however, the detection sensitivities are also not satisfactory (only at nM range), possibly because the reductant (citrates were generally used in these cases) is too weak to reduce Hg species below nM concentration in samples. In addition, some active reagents such as H_2O_2 and $NaBH_4$ in the detection system could influence the stability of AuNPs, which lowers the detection accuracy.

In the present work, we describe a novel strategy for simultaneously detecting inorganic and organic mercury with ultra-sensitivity and excellent selectivity in aqueous solution based on the cooperative effect of AuNP catalysis and Au amalgam. To realize the highly sensitive detection for Hg species, a piperazine derivative, HEPPSO i.e. N-(2-Hydroxyethyl) piperazine-N′-(2-hydroxypro-panesulfonic acid), has been specially selected and introduced to AuNPs to construct a catalysis-reduction assay for Hg species. A new AuNP-catalyzed-organic reaction is first discovered: AuNPs can catalyze HEPPSO into the catalytic product with an obvious absorption peak at about 340 nm which is used as the signal reporter for detecting Hg. HEPPSO presents a suitable reduction capacity for Hg species (such as Hg^{2+}, Hg_2^{2+} and $(CH_3)Hg^+$) to Hg°. The formation of Au amalgam by depositing Hg° atoms on AuNP surface influences the AuNP-catalyzed activities, which changes the amount of the catalytic product accompanying with the change of its absorption peak intensity at 340 nm. By using this catalysis-reduction strategy based on AuNPs, various Hg species have been simultaneously recognized at pM (ppt) range in water solution.

2. Experimental methods

2.1. Preparation of the AuNPs

The citrate-stabilized gold nanoparticles (AuNPs) with 13 nm in diameter were synthesized according to the modified Turkevich-Frens method (Turkevich et al., 1951; Frens, 1973). The citrate-stabilized AuNPs with approximate 30 nm in diameter were obtained by decreasing the amount of sodium citrate in the synthetic process of AuNPs. The morphology and size of the AuNPs were verified through transmission electron microscope (TEM) analysis. The 3101PC UV–VIS–NIR scanning spectrophotometer was used to measure the UV–Visible (UV–Vis) absorption spectra. The absorption peak of the AuNPs with the diameter at 13 and 30 nm are 519 and 525 nm, respectively. The carbonate stabilized AuNPs in diameter of approximate 6 nm were obtained by the following procedure. 1.5 mL 1% $HAuCl_4$ aqueous solution and 500 μL 0.2 M K_2CO_3 were dissolved in 100 mL water which was cooled in ice-water bath with stirring. $NaBH_4$ was dissolved in 5 mL water at a concentration of 0.5 mg/mL. 5×1 mL aliquots of fresh $NaBH_4$ solution were added to above mixture solution under the vigorous stirring. A color change from blueish-purple to raddish-orange can be observed. After stirring for 5 min in ice-water bath, AuNPs with approximate 6 nm in diameter were obtained.

2.2. Preparation of the HO-AuNPs and PH-AuNPs

To prepare the HO-AuNPs, the citrate-stabilized AuNPs in diameter of 13 nm were centrifuged twice to remove superfluous ligands, and then the stock solution of HEPPSO (25 mM, pH 7.5) was added to obtain the HO-AuNPs in water. All experiments were carried out at room temperature. Other experimental conditions, such as the solution pH, the concentration of HEPPSO or AuNPs, the AuNP size, and incubation time of HO-AuNPs, were determined by different experimental requirements. To prepare the PH-AuNPs, HO-AuNPs were added by a certain amount of Hg species in advance. Generally, after a series of optimization tests, PH-AuNPs were obtained by incubating HO-AuNPs (25 mM HEPPSO, 2.5 nM AuNPs and pH 7.5) with 0.6 μm Hg species. After incubation for 1 h, the mixture was then centrifuged and the precipitates were redissolved in the HEPPSO buffer (25 mM, pH 7.5). The freshly prepared PH-AuNPs were used to study the interaction between PH-AuNPs and Hg species or other metal ions, and the sensing sensitivity and selectivity.

2.3. The interaction of HO-AuNPs/PH-AuNPs and metal ions

To study the interaction between HO-AuNPs and mercury species, a series of 180 μL HO-AuNP solutions (2.5 nM AuNPs and 25 mM HEPPSO) with an appropriate pH (pH 7.0 or 7.5) were equilibrated at room temperature for 5 min 20 μL stock solutions of individual or mixed Hg species were then added to each of these mixtures to give the desired total Hg content (1 pM–100 μM). After incubation for 4 h, UV–Vis absorption spectra of detection solutions or their supernatants after centrifugation were recorded. For detecting Hg species, the freshly prepared PH-AuNP solutions (2.5 nM AuNPs, 25 mM HEPPSO and pH 7.5) were added to various concentrations of Hg species (1 pM–100 μM), and above experimental procedures were repeated. For studying the interactions between the freshly prepared PH-AuNPs and other metal ions (the concentration of each metal ion is 1 μM), the UV–Vis absorption spectra were recorded by the same procedures as described above. Moreover, for all quantitative experiments, before measurements the AuNPs in HO-AuNP or PH-AuNP solution were removed by centrifugation to eliminate the interference from the AuNP absorption.

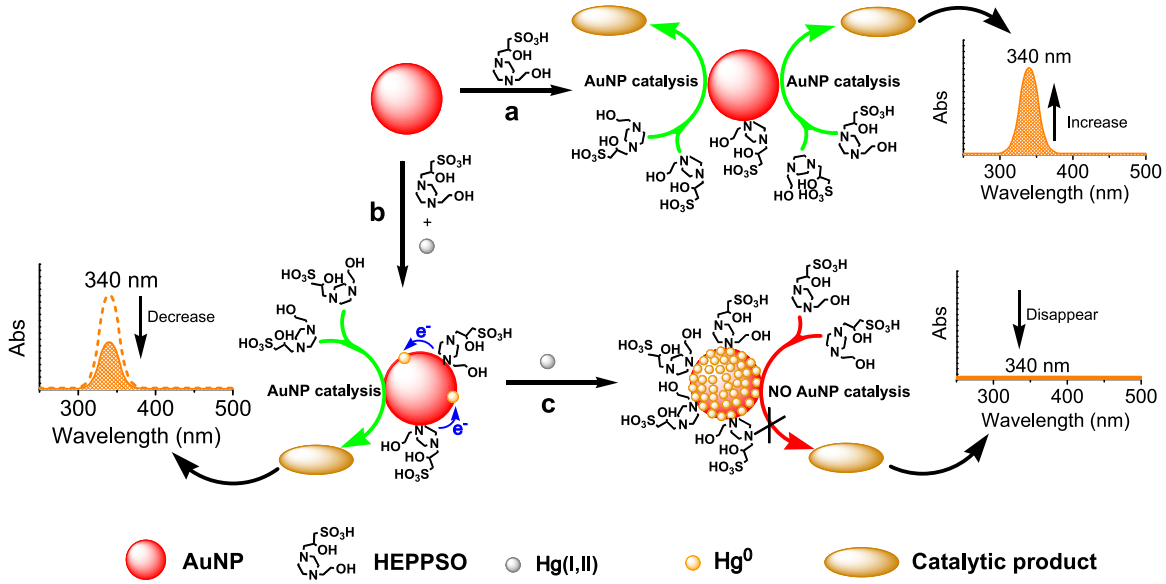

Scheme 1. Schematic representation for sensing mercury using the catalysis-reduction strategy basd on AuNPs. (a) Under AuNP catalysis, HEPPSO can be converted to the catalytic product with an obvious absorption at 340 nm. (b) With the presence of Hg(I,II), due to the formation of gold amalgam, the catalytic ability of AuNPs drops, resulting in the decrease of the absorption at 340 nm. (c) With the surface of AuNPs fully covered by Hg atoms, the catalytic capacity of AuNPs is completely inhibited and the conversion from HEPPSO to the catalytic product is completely interrupted.

3. Results and Discussion

3.1. Detection principle

In this AuNP-based assay, 13 nm AuNPs in diameter were employed to fulfill the detection performance. The catalysis-reduction strategy for the detection of Hg species is illustrated schematically in Scheme 1. In the mixed solution of AuNPs and HEPPSO, HEPPSO adsorbed on the AuNP surface can be converted to new products due to the AuNP catalysis. One of the catalytic products presents an obviously characteristic absorption peak at 340 nm (shown in Scheme 1a). With the presence of various Hg species (called as Hg(I, II) below for simplicity), Hg(I, II) can be reduced to Hg atoms (Hg^0) by HEPPSO, and then Hg^0 occupies the catalytically active sites on the surface of AuNPs by forming gold amalgam, which can lower the catalytic ability of AuNPs, leading to the decrease of amount of the catalytic product, accompanying with the decrease of its absorptive intensity at 340 nm (Scheme 1b). At last, when the surface of AuNPs is fully covered by Hg atoms, the catalytic capacity of AuNPs will be completely inhibited and the conversion from HEPPSO to the catalytic product will be interrupted (Scheme 1c). Based on that the amount of Hg deposited on AuNP surface can decrease absorption intensity of the catalytic product at 340 nm, a highly sensitive and selective assay based on catalysis-reduction strategy can be applied for the detection of Hg(I, II) content in aqueous solution.

3.2. Properties of the AuNP catalysis

A new AuNP-catalyzed-oganic reaction was first studied. Under the conditions (pH 7.5, 25 mM HEPPSO, and 13 nm AuNPs in diameter centrifuged twice), the measured UV–Vis spectra of AuNPs before and after incubation with HEPPSO solution (i.e. HO-AuNPs) are shown in Fig. 1a. Compared to the AuNP solution (red curve), HO-AuNP solution shows a new absorption peak at approximate 340 nm (black curve). Such UV–Vis absorption change suggests that new ingredient appears in the HO-AuNP solution due to the AuNP catalysis. And the catalytic ability of AuNPs could be completely blocked when the surface of AuNPs was passivated. For example, the AuNPs modified by glutathione (GSH) were incubated with HEPPSO, and the absorption intensities of UV–Vis spectra gradually decreased and eventually disappeared at 340 nm with increasing the amount of GSH on AuNP surface (Fig. 1b). This data suggest that the catalytic ability of AuNPs results from AuNP-surface properties. Moreover, the AuNP-catalyzed-organic reaction also depended on the molecule structure of catalyzing substrates. The UV–Vis spectra of AuNPs incubated with various buffer reagents with partly different structures (Fig. 1c), such as HEPPSO (containing primary and secondary hydroxyl groups, piperazine ring and sulfonic group), PIPES (no hydroxyl group), MOPSO (no primary hydroxyl group and piperazine ring), POPSO (no primary hydroxyl group), and lower aliphatic alcohols (only containing primary hydroxyl group) including methanol, ethanol, and glycerol are shown in Fig. 1d and Fig. S1. Except HEPPSO, no absorption at 340 nm appears for other similar molecules, indicating the molecules containing both primary hydroxyl group and piperazine ring can be catalyzed by AuNPs.

In addition, we have attempted to characterize the structure of the catalytic product with absorption at 340 nm by ^{13}C NMR and HPLC-ESI-MS. After the catalytic product was prepared, a yellowish-brown oily liquid was obtained, different from HEPPSO (Fig. S2 in the Supporting Information). From the obtained data of the typical ^{13}C NMR spectrum (Fig. S3 in the Supporting Information), HPLC chromatography with UV detection at 340 nm (Fig. S4 in the Supporting Information), and the mass spectra with the scan ES^+ and ES^- models (Fig. S5 and S6 in the Supporting Information), the structure of the catalytic product with the absorption peak at 340 nm contains a quaternary carbon and two acid groups (see details in the Supporting Information). We speculate that the product probably comes from condensation of two HEPPSO molecules through some AuNP-catalyzed pathway, and the possible chemical structure is shown in Fig. S7. Nevertheless, the sulfonic group maybe present in both HEPPSO and the catalytic product, which makes them have similar molecular polarity and thus the catalytic product is difficult to separate from HEPPSO. Therefore, the exact structure of the catalytic product with the absorption at 340 nm is still not sure according to the above studies. The detailed study will be done in the subsequent work.

3.3. Influencing factors of the AuNP catalysis

To achieve a satisfactory detection performance, the influencing factors of AuNP catalyzing HEPPSO to the catalytic product with

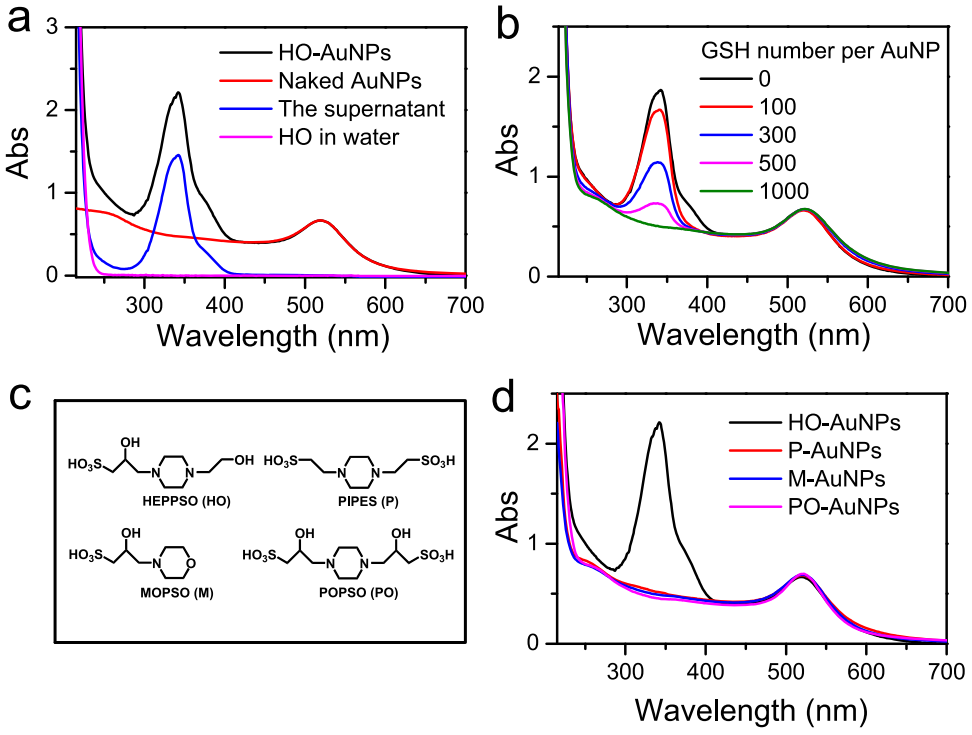

Fig. 1. (a) UV–Vis spectra of HO-AuNPs, AuNPs, the supernatant of HO-AuNPs and HEPPSO aqueous solution, respectively. (b) UV–Vis spectra of AuNPs with different amount of glutathione (GSH) per AuNP in the presence of HEPPSO. (c) The molecule structures of similar buffer reagents. (d) UV–Vis spectra of AuNPs incubated with different buffers. P-AuNPs, M-AuNPs and PO-AuNPs refer to PIPES-, MOPSO- and POPSO- modified AuNPs, respectively. The incubation conditions are 2.5 nM AuNPs, pH 7.5 and incubation time for 4 h. Buffer concentrations are 25 mM.

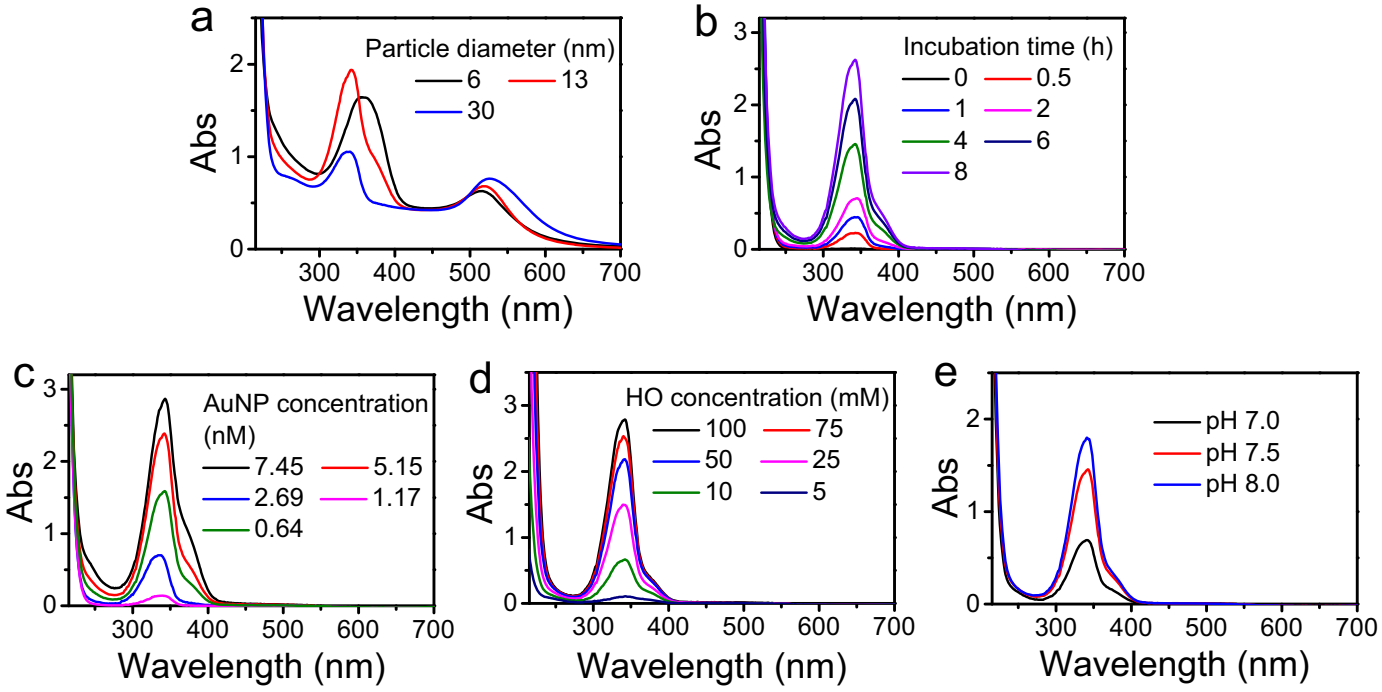

Fig. 2. UV–Vis spectra of HO-AuNPs and their supernatants after centrifuged with different incubated conditions. (a) Different diameters of AuNPs, (b) different incubated time, (c) different AuNP concentrations, (d) different HEPPSO buffer concentrations, and (e) different pH range. The other incubated conditions are 2.5 nM AuNPs (except (a)), 25 mM HEPPSO (except (c)), pH 7.5 (except (d)) and 4-h incubation time (except (b)). All experiments were done at room temperature.

absorption at 340 nm were studied by UV–Vis spectroscopy (Fig. 2). The UV–Vis spectra show that about 13 nm AuNPs in diameter have a higher catalytic activity than other particle sizes (Fig. 2a). Increasing the incubated time (Fig. 2b), the concentration of AuNPs (Fig. 2c) or HEPPSO (Fig. 2d) has the positive impact on the amount of the catalytic product, respectively. We also investigated the role of solution pH in the catalysis process (Fig. 2e). With increasing pH from 7.0 to 8.0, the absorption intensity at 340 nm increases, suggesting that hydroxyl ions can promote the catalytic process in the solution. In view of the stability of HO-AuNP solutions and appropriate detection conditions (not long-time consuming and nearly neutral condition), the catalytic conditions of this assay with 25 mM HEPPSO, 2.5 nM AuNPs

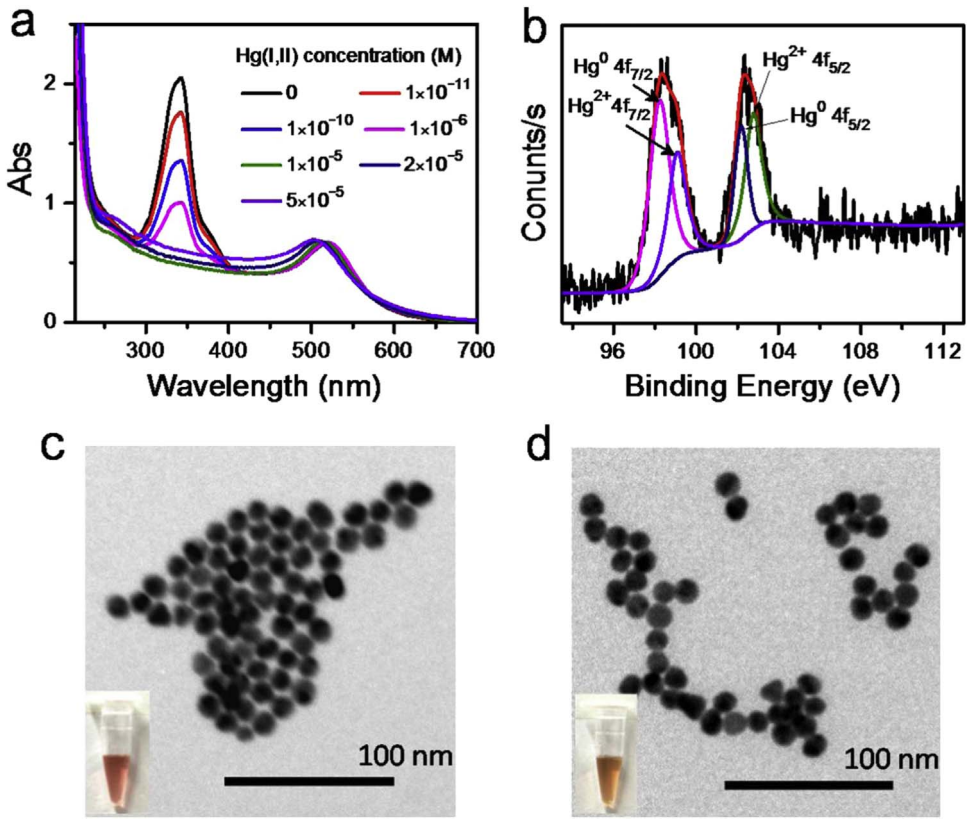

Fig. 3. (a) UV–Vis spectra of HO-AuNPs in the presence of different concentrations of Hg(I,II) (equal parts of Hg^{2+}, Hg_2^{2+} and CH_3Hg^+). The incubation conditions are 2.5 nM AuNPs, 25 mM HEPPSO, pH 7.5 and 4-h incubation time at room temperature. (b) XPS spectra of HO-AuNPs after being treated with Hg(I, II) showing the binding energy of Hg 4f. (c) TEM images of HO-AuNPs (13 nm in diameter) and (d) after treated with 50 μm Hg(I, II). Inset: the corresponding photo images of particle solution. (For interpretation of the references to color in this figure legend, the reader is referred to the web version of this article.)

(13 nm in diameter, ε=2.7×10^8 L mol^{-1} cm^{-1}) (Jin et al., 2003) and pH 7.5 were used for detecting Hg species at room temperature.

3.4. The interaction between HO-AuNPs and Hg species

To investigate the interactions between HO-AuNPs and various Hg species, under above catalysis conditions, various mercury-containing solutions, such as Hg^{2+}, Hg_2^{2+}, CH_3Hg^+ and Hg-mixed with different ratios, were added to HO-AuNPs, respectively. After incubation, their absorption intensities at 340 nm are shown in Fig. S8 in the Supporting Information. The result demonstrates that all Hg species with the same Hg content have the same effect on the decrease of the absorption intensity of catalytic product at 340 nm, indicating that the inhibition of AuNP-catalyzed activity only depends on total Hg content rather than some specific Hg species. Therefore, a mixture of various Hg species (Hg^{2+}, Hg_2^{2+} and CH_3Hg^+ are equal contents) i.e. Hg(I, II) that represents all organic and inorganic mercury were used in the following experiments. After adding various concentrations of Hg(I, II) to the freshly prepared HO-AuNPs, UV–Vis spectra were measured and shown in Fig. 3a. The absorption intensity at 340 nm gradually decreases with increasing Hg(I, II) amount. When Hg(I, II) increases to 5 μm (not given in Fig. 3a), no absorption peak can be observed at 340 nm. Meanwhile, obvious blue shift of AuNP absorption peak appears due to the amalgamation process between Hg and AuNPs.

In addition, the morphology and composition of gold amalgam were also characterized by X-ray photoelectron spectroscopy (XPS), X-ray diffraction (XRD) and transmission electron microscopy (TEM). In these cases, Hg(I, II) was added to the HO-AuNPs to obtain gold amalgam. In the XPS spectrum (Fig. S9 in the Supporting Information), both peaks corresponding to Hg 4f and Au 4f can be observed clearly. From the high resolution XPS spectrum of Hg 4f (Fig. 3b), the presence of Hg° confirms the reduction of Hg(I, II) at the AuNP surface. Moreover, from the XRD patterns (Fig. S10 in the Supporting Information), the deposition of Hg° on AuNP surface can change the crystalline degree of AuNPs, and then affects the catalytic property of AuNPs. From the TEM characterization (Fig. 3c and d), there is no obvious change for the morphology and size of particles due to the small amount of Hg deposition on AuNP surface. However, the solution color changes from red (inset of Fig. 3c) to orange-brown (inset of Fig. 3d) upon the addition of Hg(I, II), consistent with that of previous report (Henglein and Giersig, 2000). Above results suggest this assay is suitable for detecting simultaneously inorganic and organic mercury in water samples at very low concentration.

3.5. Reduction role of HEPPSO for Hg(I,II)

To confirm that it is HEPPSO but not the catalytic product for the reduction of Hg(I, II), control experiments were performed. The incubation of AuNPs with HEPPSO for some time (e.g. 4 h) generates a certain amount of the catalytic product. Then, various concentrations of Hg(I, II) were added to above HO-AuNP solution, and UV–Vis spectra are shown in Fig. S11 in the Supporting Information. Blue shifts of AuNP absorption peaks are obvious after adding Hg(I, II), consistent with the phenomena shown in Fig. 3a, which shows that Hg(I, II) has been reduced to Hg° to form the amalgamation with AuNPs. However, the absorption intensity of the catalytic product doesn't show obvious decrease by adding various concentrations of Hg(I, II), suggesting that the catalytic product cannot be consumed by Hg(I, II). Because the reductant (HEPPSO) and the signal reporter (the catalytic product) are not the same composition in the assay, the change of absorption signal at 340 nm is only decided by amount of Hg atoms (i.e. the reduced Hg(I, II)) deposited on AuNP surface, quanti-

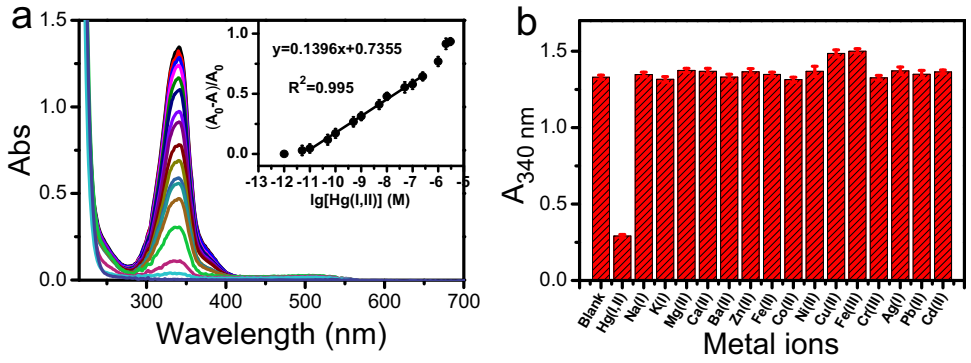

Fig. 4. (a) UV–Vis spectra of the supernatants of the pretreated HO-AuNPs (PH-AuNPs) in the presence of various Hg(I,II) content in aqueous solution. The concentrations of Hg(I, II) are 0, 1.0×10^{-12}, 5.0×10^{-12}, 1.0×10^{-11}, 5.0×10^{-11}, 1.0×10^{-10}, 5.0×10^{-10}, 1.0×10^{-9}, 5.0×10^{-9}, 1.0×10^{-8}, 5.0×10^{-8}, 1.0×10^{-7}, 2.5×10^{-7} , 1.0×10^{-6} , 2.0×10^{-6}, 3.0×10^{-6} and 1.0×10^{-5} M, from top to bottom. Inset: absorption ratio of the supernatants of the PH-AuNPs ($(A_0–A)/A_0$) as a function of the added total Hg content. The error bars are standard deviations (n=5). (b) Absorption intensities at 340 nm of the supernatants of the PH-AuNPs with various kinds of metal ions. The error bars are standard deviations (n=5). The concentrations of metal ions are 1 μm. The experimental conditions are 25 mM HEPPSO, 2.5 nM AuNPs, pH 7.5 and 4-h incubation time at room temperature.

tative analysis of Hg content can be realized.

3.6. The detection performance

To achieve sensitive and quantitative sensing of Hg(I, II), the optimal detection conditions were studied (see Fig. S12 in the Supporting Information for details). 0.6 μm Hg(I, II) was firstly pre-added into HO-AuNP solution with 2.5 nM AuNPs. The pre-treated solution was named as PH-AuNPs, which was used for the detection of Hg species in solution. The UV–Vis spectra of the freshly prepared PH-AuNPs added with various concentrations of Hg(I, II) or individual Hg species (Hg^{2+}, Hg_2^{2+} and CH_3Hg^+) are shown in Fig. 4a and Fig. S13 in the Supporting Information. The absorption intensity ratio ($(A_0–A)/A_0$) (where A_0 is the initial absorption intensity of the catalytic product and A is the absorption intensity after the addition of Hg(I, II)) shows a good linear dependence on Hg(I, II) content from 1.0×10^{-11} to 2.5×10^{-7} M, presenting a dynamic range of 5 orders of magnitude (inset of Fig. 4a). According to the decrease of the absorption intensity ratio at 340 nm, the detection limit for Hg(I, II) is as low as 5.0 pM (signal/standard deviation=3). The interactions of the PH-AuNPs with other individual Hg species also indicate that the detection effects of PH-AuNPs are in almost perfect agreement with that of the mixture of various Hg species.

In addition, we have studied the responses of PH-AuNPs for sensing Hg(I, II) with changing detection conditions (shown in Fig. S14). When the detection conditions are 5.0 nM AuNPs, 25 mM HEPPSO, pH 7.5, and 0.5-h incubation, the absorption intensity ratio vs. Hg(I, II) concentration shows the linear range from 5.0 to 1.2 μm with a detection limit of 3.0 nM. The results indicate that reducing the incubation time and increasing AuNP concentration can detect higher concentration of Hg(I, II) in nM-μM range, which falls into the US EPA limit value range, suggesting a potential practical use for real samples.

In our work, using the catalysis-reduction strategy pushes the detection limit for Hg(I, II) below at least 2 orders of magnitude than those reported by other optical methods (Chen et al., 2014a, 2014b; Lee et al., 2007; Shu et al., 2015; Chen et al., 2010; Santra et al., 2009; Lee and Mirkin, 2008; Xue et al., 2008; Liu and Lu, 2003; Zhou et al., 2008), which can be attributed to two reasons. Firstly, the appropriate reduction ability of HEPPSO can reduce all the combined states of Hg to Hg atoms at the concentration of pM range, and Hg atoms deposit on AuNP surface to form Au amalgam, which changes the features of AuNP surface. Secondly, AuNP-catalyzed detection method depends on the surface properties of AuNPs. Little amount of Au amalgam can affect the catalytic activity of AuNP and decrease the amount of the catalytic product, which causes a response-signal amplification to the Hg content in this assay. Therefore, a low detection limit for Hg at pM range can be obtained.

To evaluate the selectivity, the responses of the freshly prepared PH-AuNPs to other metal ions were studied. As expected, no significant absorption intensity change at 340 nm was observed when PH-AuNPs were incubated with other metal ions at the concentration of 1 μm (Fig. 4b and Fig. S15 in the Supporting Information). When various metal ions with the concentration at 50 μm were added to PH-AuNPs, only the detection solution containing Hg(I, II) changes to orange-brown (Fig. S16 in the Supporting Information). Some metal ions such as Cu^{2+}, Pb^{2+} and Cr^{3+} can change the solution color from red to blue, suggesting that aggregation of Au particles occurs. Competitive experiments for Hg(I, II) mixed with general co-existing metal ions also exhibited neglectable change in the absorption ratios (Fig. S17 in the Supporting Information). The results clearly indicate that the present work can specifically detect Hg(I, II). Such high selectivity for Hg detection is mainly due to the formation of gold amalgam.

To further evaluate the practical application of this method for the detection of Hg(I, II) in tap water (no Hg element was detected in drinking water by ICP-AES measurement), the analysis of Hg species was performed by adding different amounts of Hg^{2+}, Hg_2^{2+}, CH_3Hg^+ or Hg(I, II) in tap water samples (Table S1 in the Supporting Information). The recoveries of the present method can reach 96–106%. The results are consistent with those by ICP-AES method, which suggests that our method is potentially applicable to monitor all Hg species with trace or ultra-trace levels in real environmental water samples.

4. Conclusions

We have developed a novel catalysis-reduction strategy based on AuNPs for simultaneously sensing inorganic and organic mercury (Hg(I, II)) in aqueous solution with high sensitivity and selectivity. An AuNP-catalytic-organic reaction was firstly used for the detection of metal ions. HEPPSO can be converted by the AuNPs (13 nm in diameter) to the catalytic product with an absorption peak at 340 nm, which can be employed as the signal reporter for Hg(I, II). Moreover, As the reductant, HEPPSO can reduce Hg(II) to Hg atoms at the concentration of pM range. Hg atoms deposited on AuNP surface can form Au amalgam with AuNPs, which can suppress the catalytic ability of AuNPs, and thus decrease the amount of the catalytic product with the absorption signal at 340 nm. Based on the cooperative effect of AuNP catalysis and Au amalgam, the detection limit is as low as 5 pM. Moreover, the method has great potential for the application of monitoring various Hg species in environmental water samples.

Moreover, there are still two aspects that attract our interests. One is that we discovered for the first time that the compound with the

molecule structure including piperazine ring and primary hydroxyl group can be catalyzed by AuNPs at room temperature. It is necessary to investigate if there are other catalytic products, and to deeply understand the catalytic mechanism. The other point is that adding Hg species in HO-AuNPs results in an irregular change of the absorption intensity of the catalytic product. We speculate that such result may be related to the change of the surface structure of AuNPs and/or the synergistic effect of the binary metals. Further studies on these issues are currently underway.

Acknowledgements

This work was supported by the National Natural Science Foundation of China (No. 21405149, 21275136, and 11374297) and National Key Research and Development Plan (No. 2016YFA0203200). We also gratefully acknowledge Professor Xihe Bi for the assistance of the catalytic product analysis, Dr. Xiaowen Xu for the suggestions to this work, and Jianwei Wang for the assistance of the HPLC-MS data analysis.

Appendix A. Supplementary material

Supplementary data associated with this article can be found in the online version at http://dx.doi.org/10.1016/j.bios.2016.10.097.

References

Arcadi, A., 2008. Chem. Rev. 108, 3266–3325.
Bera, K., Das, A.K., Nag, M., Basak, S., 2014. Anal. Chem. 86, 2740–2746.
Boening, D.W., 2000. Chemosphere 40, 1335–1351.
Cai, S., Lao, K., Lau, C., Lu, J., 2011. Anal. Chem. 83, 9702–9708.
Chen, G.-H., Chen, W.-Y., Yen, Y.-C., Wang, C.-W., Chang, H.-T., Chen, C.-F., 2014a. Anal. Chem. 86, 6843–6849.
Chen, L., Li, J., Chen, L., 2014b. ACS Appl. Mater. Interfaces 6, 15897–15904.
Chen, X., Baek, K.-H., Kim, Y., Kim, S.-J., Shin, I., Yoon, J., 2010. Tetrahedron 66, 4016–4021.
Comotti, M., Pina, C.D., Matarrese, R., Rossi, M., 2004. Angew. Chem. Int. Ed. 43, 5812–5815.
Ding, S.-Y., Dong, M., Wang, Y.-W., Chen, Y.-T., Wang, H.-Z., Su, C.-Y., Wang, W., 2016. J. Am. Chem. Soc. 138, 3031–3037.
Du, J., Jiang, L., Shao, Q., Liu, X., Marks, R.S., Ma, J., Chen, X., 2013. Small 9, 1467–1481.
Frens, G., 1973. Nat. Phys. Sci. 241, 20–22.
Gao, Y., Shi, Z., Long, Z., Wu, P., Zheng, C., Hou, X., 2012. Microchem. J. 103, 1–14.
Henglein, A., Giersig, M., 2000. J. Phys. Chem. B 104, 5056–5060.
Hong, Y.S., Rifkin, E., Bouwer, E.J., 2011. Environ. Sci. Technol. 45, 6429–6436.
Huang, C.-C., Chang, H.-T., 2007. Chem. Commun. 12, 1215–1217.
Jensen, S., Jermelov, A., 1969. Nature 223, 753–754.
Jin, R., Wu, G., Li, Z., Mirkin, C.A., Schatz, G.C., 2003. J. Am. Chem. Soc. 125, 1643–1654.
Kim, H.N., Ren, W.X., Kim, J.S., Yoon, J., 2012. Chem. Soc. Rev. 41, 3210–3244.
Lee, J.-S., Han, M.S., Mirkin, C.A., 2007. Angew. Chem. Int. Ed. 46, 4093–4096.
Lee, J.-S., Mirkin, C.A., 2008. Anal. Chem. 80, 6805–6808.
Lehnherr, I., Louis, V.L.S., Hintelmann, H., Kirk, J.L., 2011. Nat. Geosci. 4, 298–302.
Li, X., Wang, J., Sun, L., Wang, Z., 2010. Chem. Commun. 46, 988–990.
Lien, C.-W., Tseng, Y.-T., Huang, C.-C., Chang, H.-T., 2014. Anal. Chem. 86, 2065–2072.
Liu, J., Lu, Y., 2003. J. Am. Chem. Soc. 125, 6642–6643.
Nolan, E.M., Lippard, S.J., 2008. Chem. Rev. 108, 3443–3480.
Office of Water, 2001. U.S. Environmental Protection Agency Washington, DC.
Panigrahi, S., Basu, S., Praharaj, S., Pande, S., Jana, S., Pal, A., Ghosh, S.K., Pal, T., 2007. J. Phys. Chem. C 111, 4596–4605.
Santra, M., Ryu, D., Chatterjee, A., Ko, S.-K., Shin, I., Ahn, K.H., 2009. Chem. Commun. 16, 2115–2117.
Schrope, M., 2001. Nature 409, 124.
Shu, W., Yan, L., Liu, J., Wang, Z., Zhang, S., Tang, C., Liu, C., Zhu, B., Du, B., 2015. Ind. Eng. Chem. Res. 54, 8056–8062.
Tseng, C.-W., Chang, H.-Y., Chang, J.-Y., Huang, C.-C., 2012. Nanoscale 4, 6823–6830.
Turkevich, J., Stevenson, P.C., Hillier, J., 1951. Discuss. Faraday Soc. 11, 55–75.
Wang, C.-I., Huang, C.-C., Lin, Y.-W., Chen, W.-T., Chang, H.-T., 2012. Anal. Chim. Acta 745, 124–130.
Wang, Z., Ma, L., 2009. Coord. Chem. Rev. 253, 1607–1618.
Xue, X., Wang, F., Liu, X., 2008. J. Am. Chem. Soc. 130, 3244–3245.
Yan, X.-P., Li, Y., Jiang, Y., 2003. Anal. Chem. 75, 2251–2255.
Zapata, F., Caballero, A., Espinosa, A., Tarraga, A., Molina, P., 2009. Inorg. Chem. 48, 11566–11575.
Zhang, Y., Cui, X., Shi, F., Deng, Y., 2012. Chem. Rev. 112, 2467–2505.
Zhou, Y., Wang, S., Zhang, K., Jiang, X., 2008. Angew. Chem. Int. Ed. 47, 7454–7456.